The 8th European Congress on Computational Methods in Applied Sciences and Engineering
ECCOMAS Congress 2022
5-–9 June 2022, Oslo, Norway

THE X-MESH METHOD APPLIED TO MULTIPHASE FLOWS

A. QUIRINY[1], J-F. REMACLE[1], J. LAMBRECHTS[1] AND N. MOËS[2,3]

[1] Institute of Mechanics, Materials and Civil Engineering (iMMC)
Université catholique de Louvain
Avenue Georges Lemaître 4, 1348 Louvain-la-neuve, Belgium
{antoine.quiriny, jean-francois.remacle, jonathan.lambrechts}@uclouvain.be

[2] Nantes Université, École Centrale de Nantes
1, rue de la Noë, 44321 Nantes, France
nicolas.moes@ec-nantes.fr

[3] Institut Universitaire de France (IUF)

Key words: Two-phase Flows, Interface, FEM

Abstract. The accurate modeling of moving boundaries and interfaces is a difficulty present in many situations in computational mechanics. In this paper we use a new approach, X-Mesh, to simulate with the finite element method the interaction between two immiscible fluids while keeping an accurate description of the interface without mesh regeneration. The method is validated with complex problems such as Rayleigh-Taylor instabilities, sloshing and dambreak. The quality of the results and the efficiency of the method show the potential of this approach to simulate such physical phenomena.

1 Introduction

Many physical problems present discontinuities that need to be well modeled in order to be simulated correctly, one of them are the two-phase flows. The study of these flows covers a wide variety of engineering and environmental flows, such as open channel flows, wave dynamic, flow past a structure etc. The interaction between the two fluids is characterized by an interface, on which the material properties such as viscosity or density are discontinuous. The accurate representation of this interface is the main challenge for solving time-dependent two-phase flows.

Several computational methods have been developed to model this interface and can be separated in two categories: the front tracking methods including the Arbitrary Lagrangian-Eulerian (ALE) method [5] and the front capturing methods notably with the level set method (LS) [3] and diffuse level set methods (DLS) [2][4]. Although they all have interesting advantages, the existing methods still have some drawbacks: inability to take into account large movements of the interface as well as topology changes (ALE), loss of simplicity and robustness of the classical finite element method (LS), over-diffusion of the interface (DLS), ... Very recently, a new interface tracking method named X-Mesh has been developed and tested for the simulation of

a phase-change with the Stefan model [1]. The idea is similar to the ALE method but instead of positioning always the same nodes on the interface, the X-Mesh method deforms the mesh while keeping the same connectivity, creating almost degenerated elements, to allow the relay of the interface between the nodes.

This paper is structured as follows: we first present the governing equations for the two-phase flows. Then we describe the numerical methods used to solve theses equations: the Navier-Stokes solver, the advection of the level set, the algorithm used to deform the mesh and make it correspond to the interface at any time step (X-Mesh) and the coupling between the different solvers and X-Mesh. Finally the numerical results are presented, along with a discussion.

2 Governing Equations

We consider the laminar flow of two non-miscible incompressible and newtonian fluids in two dimensions. The two fluid phases are denoted Ω_1 and Ω_2 as shown at Fig 1 and have different density and kinematic viscosity : (ρ_1, ν_1) and (ρ_2, ν_2). The incompressible Navier-Stokes equations solved simultaneously on the two subdomain are given by:

$$\begin{aligned} \partial_t \mathbf{u} + \mathbf{u} \cdot \nabla \mathbf{u} &= -\nabla p + \nu \nabla^2 \mathbf{u} + \mathbf{f} \\ \nabla \cdot \mathbf{u} &= 0 \end{aligned} \tag{1}$$

where $\mathbf{u}$ is the velocity field $(u, v)^T$, p is the kinematic pressure (i.e. pressure divided by density ρ), $\mathbf{f}$ the forces at distance (gravity) and ν the kinematic viscosity.

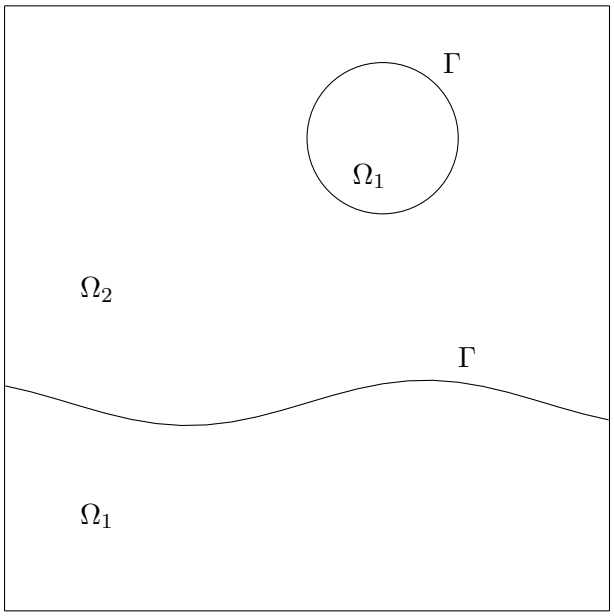

Figure 1: Two-fluid flow sketch

Since the two-fluids are non-miscible, we consider the interface Γ as impermeable such that

no mass transfer is allowed between the two phases. This leads to the condition of a continuous velocity at the interface:

$$[\mathbf{u}] = \mathbf{0}$$

where the brackets refer to the jump at the interface.
Another condition is the conservation of the momentum in the direction perpendicular to the interface. To satisfy this condition, the jump in normal stress is balanced by the surface tension:

$$[-pI + \nu\nabla\mathbf{u}] \cdot \mathbf{n} = \sigma\kappa\mathbf{n}$$

with I the identity operator, σ the surface tension coefficient and κ the curvature of the interface. In the examples treated in this paper, the effects of the surface tension can be neglected and thus σ is set to 0.

The position of the interface is determined by the zero iso-contour of a level set function ϕ. This function corresponds to a signed distance to the interface which is negative in one phase and positive in the other. The time evolution of the interface is obtained by the level set equation:

$$\partial_t\phi + \mathbf{u} \cdot \nabla\phi = 0 \tag{2}$$

with $\mathbf{u}$ corresponding to the velocity of the fluids obtained in equations 1.

3 Numerical method

In this section we describe our numerical method for the resolution of two-phase flows. We choose to work with the finite element method and more specifically with the continuous Galerkin approach and stabilized P1 elements for solving both the level set equation 2 and the Navier-Stokes equations 1. The algorithm to deform the mesh in order to follow the interface is then explained in section 3.3. Finally, an iterative coupling between these steps is presented.

3.1 Navier-Stokes solver

The considered flows are dominated by the advection and the continuous Galerkin need to be stabilized, we do it here with an additional Streamline Upwind/Petrov-Galerkin (SUPG) term. To limit the size of the system of equation that we need to solve, the unknowns are placed at the nodes of our triangular mesh both for the pressure and the velocity field. This doesn't satisfy the Babuska-Brezzi condition and could lead to the apparition of spurious mode that need to be stabilized. This problem is overcome thanks to the popular Pressure-Stabilizing/Petrov-Galerkin (PSPG) method [6]. For the mesh to permanently match the interface, the nodes are continuously moved in the computational space. This displacement is taken into account in the resolution with a non-conservative Arbitrary Lagrangian-Eulerian (ALE) formulation which consists in subtracting the mesh velocity $\mathbf{u}_{mesh}$ in the advective term. Time can be discretize with a constant time step Δt and the mesh velocity is considered piecewise constant $\mathbf{u}_{mesh} = (\mathbf{x}_{n+1} - \mathbf{x}_n)\frac{1}{\Delta t}$. We denote the value of a variable at time $t = n\Delta t$ with the subsript $\cdot_n$. The computational domain is also evolving during time, the domain at time step n is thus noted Ω^n. For the temporal integration we use the implicit euler scheme and we obtain the

semi-discrete weak formulation with the finite element method.
Consider $\mathbf{S}_{\mathbf{u}}^h$ and $\mathbf{S}_p^h$, the solution spaces of $\mathbf{u}_{n+1}$ and p_{n+1} respectively and their test functions $\left(\mathbf{v}_{n+1}^h, q_{n+1}^h\right) \in \mathbf{V}_{\mathbf{u}}^h \times \mathbf{V}_p^h$.

Find $\left(\mathbf{u}_{n+1}^h, p_{n+1}^h\right) \in \mathbf{S}_{\mathbf{u}}^h \times \mathbf{S}_p^h$ such that for any $\left(\mathbf{v}_{n+1}^h, q_{n+1}^h\right) \in \mathbf{V}_{\mathbf{u}}^h \times \mathbf{V}_p^h$:

$$\left(\int_{\Omega^{n+1}} \mathbf{u}_{n+1}^h \cdot \mathbf{v}_{n+1}^h d\Omega - \int_{\Omega^{n+1}} \mathbf{u}_n^h \cdot \mathbf{v}_{n+1}^h d\Omega\right) \frac{1}{\Delta t} + \int_{\Omega^{n+1}} \left(\left(\mathbf{u}_{n+1}^h - \mathbf{u}_{mesh}\right) \cdot \nabla \mathbf{u}_{n+1}^h\right) \cdot \mathbf{v}_{n+1}^h d\Omega$$
$$+ \nu \int_{\Omega^{n+1}} \nabla \mathbf{u}_{n+1}^h : \nabla \mathbf{v}_{n+1}^h d\Omega - \int_{\Omega^{n+1}} p_{n+1}^h \left(\nabla \cdot \mathbf{v}_{n+1}^h\right) d\Omega$$
$$= \int_{\Omega^{n+1}} \mathbf{f}_{n+1} \cdot \mathbf{v}_{n+1}^h d\Omega + \int_{\partial\Omega_N^{n+1}} \mathbf{t}_{n+1} \cdot \mathbf{v}_{n+1}^h ds + \mathrm{SUPG}_{n+1} + \mathrm{PSPG}_{n+1}$$

$$\int_{\Omega^{n+1}} q_{n+1}^h \left(\nabla \cdot \mathbf{u}_{n+1}^h\right) d\Omega = 0$$

With SUPG_{n+1} the term for the SUPG stabilization and PSPG_{n+1} the term from the PSPG stabilization.

The classical finite element spatial discretization yields a nonlinear system of equations for $\mathbf{u}_{n+1}^h$ and p_{n+1}^h; this system is solved using the Newton-Raphson method.

3.2 Advection of the level set

The position of the interface between the two fluids is considered as the iso-zero contour of a level set function. The time evolution of the level set is obtain by equation 2. This equation is stabilized with a SUPG term, the mesh displacement is managed with a conservative ALE formulation and time integration is solved by a Crank-Nicholson scheme. This formulation make appear an intermediate computation domain $\Omega^{n+\frac{1}{2}}$ that can be approximate as the mean of Ω^n and Ω^{n+1} since we consider piecewise constant mesh velocity. Let $\mathbf{S}_\phi^h$ be the solution space of ϕ_{n+1} and $w_{n+1}^h \in \mathbf{V}_\phi^{\mathbf{h}}$ be the test function associated to ϕ_{n+1}. The weak semi-discrete formulation, where the ALE formalism makes a second term appear in the advection, can then be written as follows:

Find $\phi_{n+1}^h \in \mathbf{S}_\phi^h$ such that for any $w_{n+1}^h \in \mathbf{V}_\phi^{\mathbf{h}}$:

$$\frac{1}{\Delta t}\left(\int_{\Omega^{n+1}} \phi_{n+1}^h \hat{w}_{n+1} d\Omega - \int_{\Omega^n} \phi_n^h \hat{w}_n d\Omega\right)$$
$$+ \frac{1}{2}\left(\int_{\Omega^{n+\frac{1}{2}}} \left(\mathbf{u} - \mathbf{u}_{mesh}\right) \cdot \nabla \phi_n^h \hat{w}_{n+\frac{1}{2}} d\Omega + \int_{\Omega^{n+\frac{1}{2}}} \phi_n^h \nabla \cdot \left(\mathbf{u} - \mathbf{u}_{mesh}\right) \hat{w}_{n+\frac{1}{2}} d\Omega\right)$$
$$+ \frac{1}{2}\left(\int_{\Omega^{n+\frac{1}{2}}} \left(\mathbf{u} - \mathbf{u}_{mesh}\right) \cdot \nabla \phi_{n+1}^h \hat{w}_{n+\frac{1}{2}} d\Omega + \int_{\Omega^{n+\frac{1}{2}}} \phi_{n+1}^h \nabla \cdot \left(\mathbf{u} - \mathbf{u}_{mesh}\right) \hat{w}_{n+\frac{1}{2}} d\Omega\right) = 0$$

with $\hat{w}_n = w_n - \tau_{\mathrm{SUPG}} \left(\mathbf{u} - \mathbf{u}_{mesh}\right) \cdot \nabla w_n$ the test function modified by the SUPG method in the domain Ω_n and $\hat{w}_{n+1}$ and $\hat{w}_{n+\frac{1}{2}}$ the modified test function in Ω_{n+1} and $\Omega_{n+\frac{1}{2}}$ respectively.

The finite element method then allows us to spatially discretize the domain and we obtain a linear equation system.

3.3 X-Mesh

The idea behind the X-Mesh method [1] is to deform a mesh of fixed topology with continuous node movements to constantly match the interfaces of interest, even in the case of topological changes of the fluids domains. To achieve this goal, the method allows elements to become degenerate, meaning that a triangle can deform down to an edge or even a point. This enables the mesh to deform continuously in time and ensure the relay of the front. The interface is transferred from one node to another located at the same position allowing the interface to propagate like a relay race.

Figure 2 illustrates the method used to move the nodes so that the mesh conforms to the interface defined by the level set. In this simplified example, we consider a horizontal interface and the evolution of the interface governed by the resolution of equation 2 provides us with a new level set such that the interface has been rotated by -20°. Because the deformation of the mesh is local and only affects the elements close to the interface, the first step is to determine which nodes will potentially move. These are the nodes that were part of the front at the previous time step as well as the nodes whose level set value has changed sign. These nodes are called active nodes and are marked in yellow in figure 2 (b). In our example, the old nodes of the front (marked in black in figure 2 (a)) on the horizontal line as well as two nodes that have changed sign between the two level sets are noted as active nodes. In the second step, we list the potential targets of each active node, i.e. the positions where the active nodes could be placed to be on the interface. There is an infinity of possible positions for each node but we limit ourselves to move the nodes only along their edges in order to avoid inverted elements. We also do not consider edges that connect two active nodes. These targets are then the 0 value positions of the interpolated level set on the edges connecting an active node to an inactive one. They are represented in black and white on figure 2 (c). The third step consists simply in choosing as new position of the active node its closest target and this way obtain the new mesh as shown in figure 2 (d) which is conformal to the new interface. The active nodes that have been moved form the new front and all the other nodes are relaxed towards their initial position ie. they are progressively moved to return to their initial position over several time steps.

3.4 Coupling

Algorithm 1 describes a simple iterative coupling between the fluid solver and the interface repositioning for one time step. For each iteration, the Navier-Stokes equations are solved via a Newton-Raphson solver and we obtain $\mathbf{u}_n$. This velocity will then be used in the resolution of the level set advection equation. For each intermediate solution ϕ_i, the mesh is moved to take into account the displacement of the interface. This displacement of the nodes induces a mesh velocity which must be taken into account in the resolution of the Navier-Stokes equations and the level set advection. It is then necessary to iterate until convergence for the position of the interface and thus for the mesh velocity or until it reaches the maximal number of iteration. When simulating a time step from n to $n+1$, we thus have two meshes Ω^n and Ω^{n+1} which are

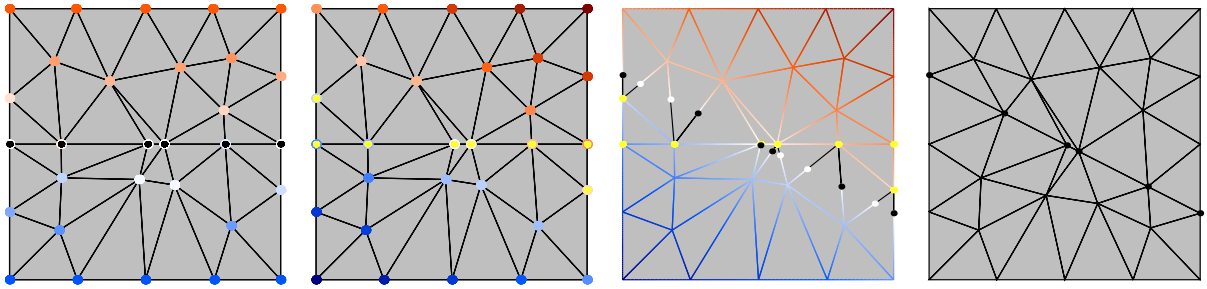

(a) Old level set values (b) New level set values (c) Potential targets (d) New mesh

Figure 2: Mesh deformation algorithm for X-Mesh [1]

consistent with the interface at both times n and $n+1$.

Algorithm 1 Coupling for a time step

$\mathbf{u}_{n+1} = \mathbf{u}_n$
$\phi_{n+1} = \phi_n$
$\mathbf{x}_{n+1} = \mathbf{x}_n$
$i = 0$
while $|\Delta \mathbf{x}| <$ tol **and** $i <$ iter **do**
  $\mathbf{u}^{\text{mesh}} = (\mathbf{x}_{n+1} - \mathbf{x}_n)\,\frac{1}{\Delta t}$
  $\mathbf{u}_{n+1} =$ Navier-Stokes $\left(\mathbf{u}_n, \phi_{n+1}, \mathbf{u}^{\text{mesh}}\right)$
  $\Delta\phi =$ LevelSet $\left(\mathbf{u}_{n+1}, \mathbf{u}^{\text{mesh}}, \phi_n\right) - \phi_{n+1}$
  $\Delta \mathbf{x} =$ X-Mesh $\left(\mathbf{x}_{n+1}, \phi_{n+1}, \Delta\phi\right) - \mathbf{x}_{n+1}$
  $\phi_{n+1} = \phi_{n+1} + \Delta\phi$
  $\mathbf{x}_{n+1} = \mathbf{x}_{n+1} + \Delta x$
  $i = i + 1$
end while

4 Results

In this section, we present the different results obtained with our approach. The first test case consists of low amplitude sinusoidal sloshing. This problem could be easily realized with a classical ALE method and does not use the advantage of X-Mesh to allow large deformations and topology changes but it has the advantage of having an analytical solution. It is therefore a good first problem to validate our implementation. The test cases of the dam break and Rayleigh Taylor instability will further validate the approach used and the interest of the method in the case of two-phase flow but also highlight some weak points that need to be addressed.

4.1 Sloshing

In order to validate our implementation, we started with a simple sinusoidal sloshing problem. It consists of the observation of the free oscillation of a liquid and especially the frequency of

the wave. The sloshing of fluids is a really practical problem for many engineering applications. We consider periodic boundary conditions on the sides and no slip conditions for the bottom and the top. An analytical solution exists for the linearized equation and is exact at the limit when the wave amplitude and the viscosity tend to zero. The effect of the top and bottom sides of the tank are negligible if we consider the deep water approximation. To compare correctly different initial conditions with the analytical solution, we consider the following conditions:

$$\frac{H}{gT^2} = 1 \cdot 10^{-1} \qquad \text{(Deep water)}$$
$$\frac{h}{gT^2} = 5 \cdot 10^{-4} \qquad \text{(Small perturbation)}$$

where λ is the wavelength, ν is the viscosity, H is the depth, h is the perturbation height and T is the theoretical period of oscillation.
Table 1 presents the experimental and theoretical wave speeds. The density and viscosity ratio considered are $\frac{\rho_1}{\rho_2} = \frac{\nu_1}{\nu_2} = 10$. As the viscosity decreases the simulations are more and more close to the linear solution, which corresponds well to the hypothesis of negligible viscosity. The error become quickly negligible for low viscosity fluids. The perturbation of this problem are so small

Table 1: Wave speed c for different values of wave number k and viscosity.

k	$\nu \cdot 10^{-3}$	c	c_{th}	error
2π	3.13	1.094	1.13	3.19%
6π	0.602	0.641	0.653	1.84%
2π	0.602	1.118	1.13	1.06%
2π	0.0602	1.13	1.13	0.022%

that the relay of the front between the element almost doesn't appear and it could easily be solved with classical ALE. This test allow us to validate our implementation of the Navier-Stokes solver, the resolution of the level set equation and the mesh deformation with X-Mesh.

To validate our approach we tested it with two more complex however classical benchmark problems for two-phase flows: a dambreak and Rayleigh-Taylor instabilities.

4.2 Dambreak

In this problem a column of dense fluid of size 0.4m by 0.4m is placed in a container of size 1.4m by 1.4m filled with a lighter fluid. The column collapses brutally and can be compared to

a sudden failure of a dam. The properties of the considered fluids are

$$\rho_1 = 1000 \quad \left[\frac{kg}{m^3}\right]$$
$$\rho_2 = 1 \quad \left[\frac{kg}{m^3}\right]$$
$$\nu_1 = \nu_2 = 1 \cdot 10^{-3} \quad \left[\frac{m^2}{s}\right]$$

Figure 3 shows the results at different time steps where t is expressed in seconds. As we can see at $t = 1.15$ we have a change in the phase topology which is naturally taken into account by the level set. The mesh deformation is shown in Figure 4, the nodes are positioned so that the mesh matches the interface at any time. As we can see in the close view of Figure 4 (b), some elements are almost degenerated. To avoid the bad conditioning of the matrix, there is a minimum limit for the value of the determinant. In practice, this value is rarely reached by the deformed elements. The X-Mesh algorithm presented in section 3.3 has the advantage of being based on the mesh topology. This allows us to have a finer initial mesh in the zone of interest like the one presented in Figure 4 (a).

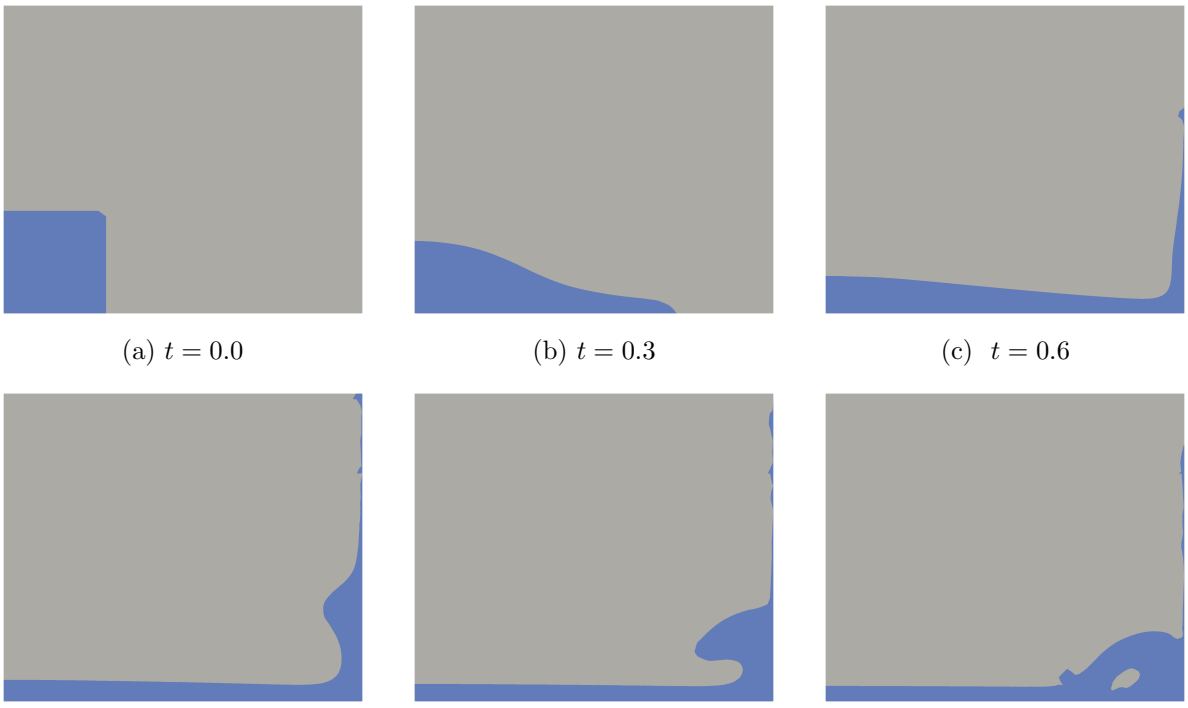

(a) $t = 0.0$ (b) $t = 0.3$ (c) $t = 0.6$

(d) $t = 0.9$ (e) $t = 1.05$ (f) $t = 1.15$

Figure 3: Simulation of a viscous dambreak

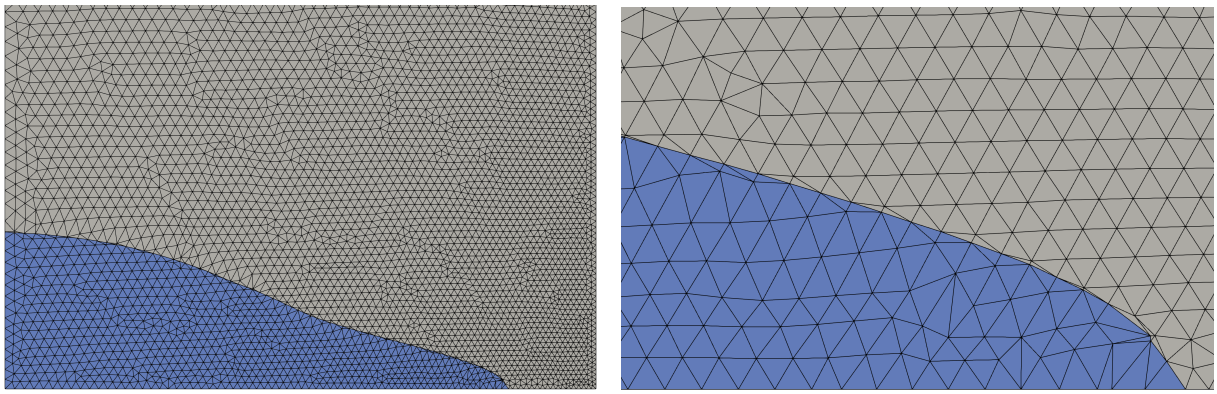

(a) Resolution mesh of the dambreak (b) Close view of the mesh deformation

Figure 4: Computational mesh for a dambreak simulation

4.3 Rayleigh-Taylor instability

Rayleigh-Taylor instability consist in placing a heavier fluid above a lighter one. This position is an unstable equilibrium and is sensible to any perturbation. A disturbance is initialized in the interface position at $t = 0$ and it's initial position is given by:

$$y = 2.0 + 0.05 \cos 2\pi x$$

The initial velocity field is zero, pressure field is hydrostatic and all the boundary conditions are free slip. The phenomenon is driven by the Atwood number $\mathrm{At} = (\rho_1 - \rho_2)/(\rho 1 + \rho 2)$ and the Reynolds number that correspond in this context to $Re = \sqrt{Wg}W/\nu$ with W the width of the channel. Figure 5 shows the results for $\mathrm{At} = 0.5$ and $\mathrm{Re} = 256$ at different adimensional time steps $t_{adim} = t\sqrt{g/W}$. The preservation of the symmetry of the interface and its smoothness is surprisingly good. These results are similar to the simulation obtained by He et al. [8]. We observe on Figure 5 (i) a mass loss due the bad capturing of the interface in the zone of strong curvature. When the curvature is so strong that a triangle has it's three nodes positioned on the interface, the phase of this element is ambiguous: two different interfaces are possible. The criteria for determining the phases of such triangle still need to be improved. In order to limit the impact of these ambiguous elements on the simulation one could also refine the mesh.
An analytical solution for the linearized equations exist and is valid for the linear phase of the instability development [9]:

$$h = h_0 e^{\hat{\alpha} t}$$

with h the perturbation size, h_0 the perturbation at $t = 0$ and $\hat{\alpha}$ the growth rate. For the parameter of the simulation the analytical grow rate is $\hat{\alpha}_a = 9.3$ and the observed one is $\hat{\alpha}_o = 9.2$.

5 Conclusion

A mesh conforming approach for the numerical simulation of 2D two-phase flows has been presented. This approach relies on a classical implicit stabilized finite element solver for the

Navier-Stokes equations, a stabilized finite element approximation for the resolution of the level set equation and a local mesh adaptation method, X-Mesh, that accurately tracks the interface. The main advantage is the simple representation of the sharp interface between the two fluids without the need of remeshing and thus no mesh topology change. This representation allows the capturing of the discontinuities in the derivatives of our variables which can not be done in classical eulerian level set methods. In contrast with the classical ALE method, by tracking the front with the nodes successively in the way of a relay race, the X-Mesh method allows to track interface with movement of large amplitude and phase topology change. Thanks to the local aspect of the bad-shaped elements, the quality of the solution is preserved. By limiting the minimum value of the determinant of the almost degenerated elements we avoid the bad conditioning of the finite element matrix.

The preliminary results presented here are in good agreement with the analytical solutions and the literature. This is encouraging for the use of the X-Mesh method in such challenging computational mechanics problem. For future applications we will focus on the implementation of the surface tension. Having the nodes of the mesh positioned exactly on the interface should be an advantage for the application of this force.

REFERENCES

[1] N. Moës, J.-F. Remacle, J. Lambrechts, and B. Lé, The eXterme Mesh deformation approach (X-MESH) for the Stefan phase-change model. *http://arxiv.org/abs/2111.04179* (2021)

[2] M. Sussman, E. Fatemi, An efficient interface preserving level set redistancing algorithm and its application to interfacial incompressible fluid flow, *SIAM Journal on Scientific Computing* (1999) **20**:1165-1191.

[3] E. Marchandise, J.-F. Remacle, A stabilized finite element method using a discontinuous level set approach for solving two phase incompressible flows, *Journal of Computational Physics* (2006) **219**:780-800

[4] S. Nagrath, K. Jansen, R. Lahey, Computation of incompressible bubble dynamics with a stabilized finite element level set method, *Computer Methods in Applied Mechanics and Engineering* (2005) **194 (42-44)**:4565-4587

[5] T. Hughes, W. Liu, T. Zimmermann, Lagrangian-Eulerian finite element formulation for incompressible viscous flows, *Computer Methods in Applied Mechanics and Engineering* (1981) **29**:239-349

[6] T. Hughes, L.P Franca, A new finite element formulation for computational fluid dynamics: V. circumventing the Babuska-Brezzi condition: A stable Petrov-Galerkin formulation of the stokes problem accommodating equal-order interpolations, *Computer Methods in Applied Mechanics and Engineering* (1986) **59**:85-99

[7] A.N. Brooks and T. Hughes, Streamline Upwind/Petrov Galerkin formulations for convection dominated flows with particular emphasis on the incompressible Navier-Stokes equations. *Computer Methods in Applied Mechanics and Engineering* (1982) **32**:199-259

[8] Xiaoyi He, Shiyi Chen and Raoyang Zhang, A Lattice Boltzmann Scheme for Incompressible Multiphase Flow and its Application in Simulation of Rayleigh-Taylor Instability *Journal of Computational Physics* (1999) **152**:642-663

[9] P. G. Drazin and W. H. Reid, Hydrodynamic stability (2004) Cambridge university press.

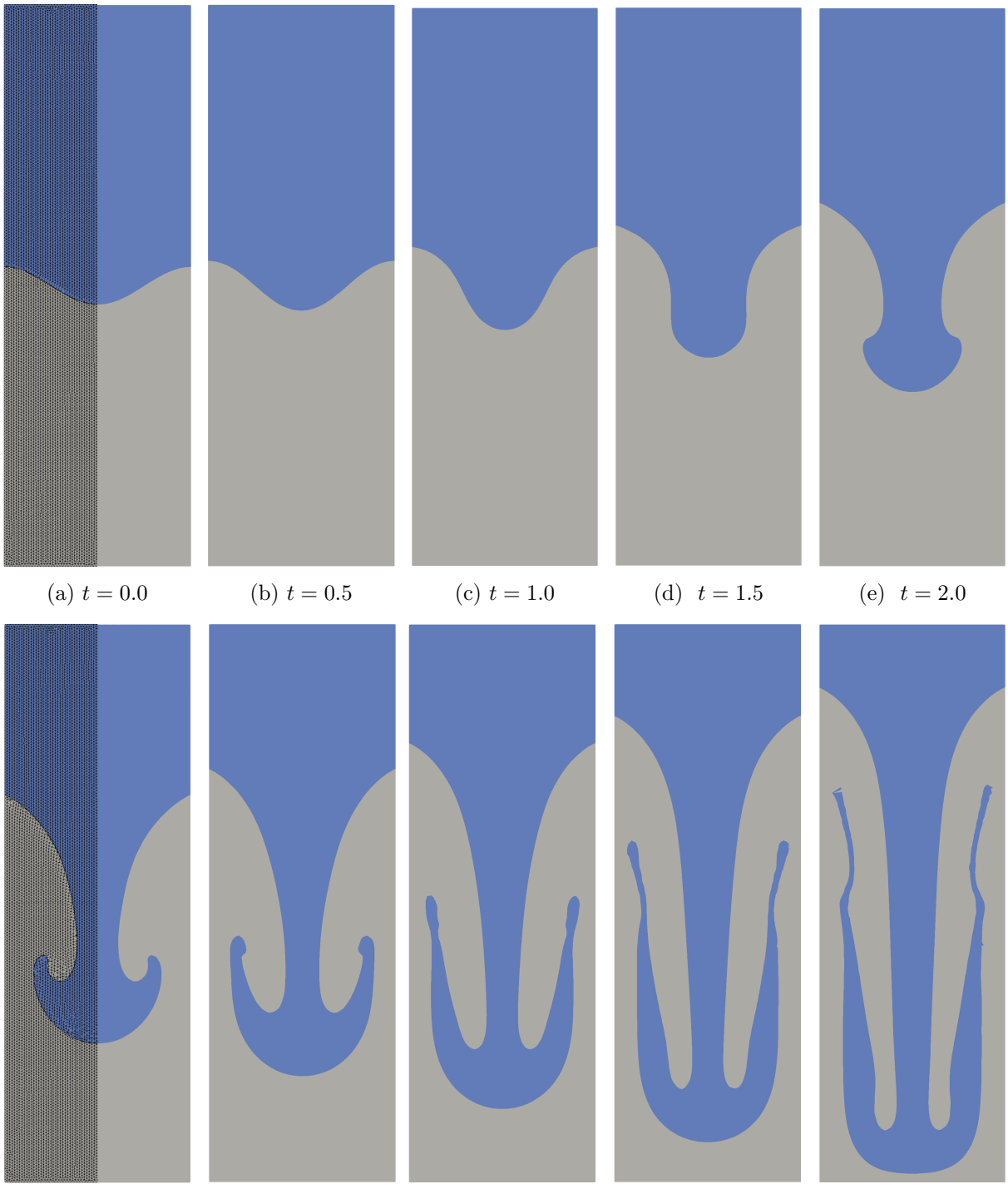

(a) $t = 0.0$ (b) $t = 0.5$ (c) $t = 1.0$ (d) $t = 1.5$ (e) $t = 2.0$

(f) $t = 2.5$ (g) $t = 3.0$ (h) $t = 3.5$ (i) $t = 4.0$ (j) $t = 4.5$

Figure 5: Rayleigh-Taylor instability for At $= 0.5$ and Re $= 256$ at different adimensional times $t_{adim} = t\sqrt{g/W}$